THE JOURNAL OF BIOLOGICAL CHEMISTRY VOL. 283, NO. 19, pp. 13044–13052, May 9, 2008

The Cytoplasmic Loops of Subunit *a* of *Escherichia coli* ATP Synthase May Participate in the Proton Translocating Mechanism*[S]

Received for publication, February 4, 2008 Published, JBC Papers in Press, March 12, 2008, DOI 10.1074/jbc.M800900200

Kyle J. Moore, Christine M. Angevine, Owen D. Vincent, Brian E. Schwem, and Robert H. Fillingame[1]

From the Department of Biomolecular Chemistry, School of Medicine and Public Health, University of Wisconsin, Madison, Wisconsin 53706

Subunit *a* plays a key role in promoting H^+ transport and the coupled rotary motion of the subunit *c* ring in F_1F_0-ATP synthase. H^+ binding and release occur at Asp-61 in the middle of the second transmembrane helix (TMH) of F_0 subunit *c*. H^+ are thought to reach Asp-61 via aqueous pathways mapping to the surfaces of TMHs 2–5 of subunit *a* based upon the chemical reactivity of Cys substituted into these helices. Here we substituted Cys into loops connecting TMHs 1 and 2 (loop 1–2) and TMHs 3 and 4 (loop 3–4). A large segment of loop 3–4 extending from loop residue 192 loop to residue 203 in TMH4 at the lipid bilayer surface proved to be very sensitive to inhibition by Ag^+. Cys-161 and -165 at the other end of the loop bordering TMH3 were also sensitive to inhibition by Ag^+. Further Cys substitutions in residues 86 and 93 in the middle of the 1–2 loop proved to be Ag^+-sensitive. We next asked whether the regions of Ag^+-sensitive residues clustered together near the surface of the membrane by combining Cys substitutions from two domains and testing for cross-linking. Cys-161 and -165 in loop 3–4 were found to cross-link with Cys-202, -203, or -205, which extend into TMH4 from the cytoplasm. Further Cys at residues 86 and 93 in loop 1–2 were found to cross-link with Cys-195 in loop 3–4. We conclude that the Ag^+-sensitive regions of loops 1–2 and 3–4 may pack in a single domain that packs at the ends of TMHs 3 and 4. We suggest that the Ag^+-sensitive domain may be involved in gating H^+ release at the cytoplasmic side of the aqueous access channel extending through F_0.

The H^+-transporting F_1F_0-ATP synthases of oxidative phosphorylation utilize the energy of a transmembrane electrochemical gradient of H^+ or Na^+ to mechanically drive the synthesis of ATP via two coupled rotary motors in the F_1 and F_0 sectors of the enzyme (1–3). In the intact enzyme, ATP synthesis or hydrolysis takes place in the F_1 sector at the surface of the membrane with synthesis coupled to H^+ transport through the transmembrane F_0 sector. Homologous enzymes are found in mitochondria, chloroplasts, and many bacteria (4). In *Escherichia coli* and other eubacteria, F_1 consists of five subunits in an $\alpha_3\beta_3\gamma_1\delta_1\epsilon_1$ stoichiometry (4). F_0 is composed of three subunits in a likely ratio of $a_1b_2c_{10}$ in *E. coli* and *Bacillus subtilis* PS3 or $a_1b_2c_{11}$ in the Na^+-translocating *Ilyobacter tartaricus* ATP synthase (3, 5–7) and may contain as many as 15 *c* subunits in other bacterial species (8). Subunit *c* spans the membrane as a helical hairpin with the first TMH[2] on the inside and the second TMH on the outside of the *c* ring (7, 9, 10). A high resolution x-ray structure of the *I. tartaricus* c_{11} ring has revealed the sodium binding site at the periphery of the ring with chelating groups to the Na^+ extending from two interacting subunits (7). The essential *I. tartaricus* Glu-65 in the Na^+-chelating site corresponds to *E. coli* Asp-61. In the H^+-transporting *E. coli* enzyme, Asp-61 at the center of the second TMH is thought to undergo protonation and deprotonation as each subunit of the *c* ring moves past a stationary subunit *a*. In the complete membranous enzyme, the rotation of the *c* ring is proposed to be driven by H^+ transport at the subunit *a*/*c* interface with ring movement then driving rotation of subunit γ within the $\alpha_3\beta_3$ hexamer of F_1 to cause conformational changes in the catalytic sites leading to synthesis and release of ATP (1–3).

Subunit *a* folds in the membrane with five TMHs and is thought to provide access channels to the proton-binding Asp-61 residue in the *c* ring (11–14). Interaction of the conserved Arg-210 residue in *a*TMH4 with *c*TMH2 is thought to be critical during the deprotonation-protonation cycle of *c*Asp-61 (15–17), and *a*TMH4 and *c*TMH2 are known to pack in parallel to each other based upon cross-linking (18). Little is known about the structure or three-dimensional arrangement of the TMHs in subunit *a*. Based initially upon the position of several sets of second site suppressor mutations, we recently introduced pairs of Cys into putatively apposing TMHs and tested for zero-length cross-linking with disulfide bond formation (19). Cross-links were found with eight different Cys pairs and define a juxtaposition of TMHs 2–3, 2–4, 2–5, 3–4, 3–5, and 4–5 packing in a four-helix bundle (19).

The differential reactivity of cysteines introduced by site-directed mutagenesis has been used as a means of probing

* This work was supported, in whole or in part, by National Institutes of Health Grant GM23105 from the United States Public Health Service. The costs of publication of this article were defrayed in part by the payment of page charges. This article must therefore be hereby marked "*advertisement*" in accordance with 18 U.S.C. Section 1734 solely to indicate this fact.

[S] The on-line version of this article (available at http://www.jbc.org) contains a supplemental table summarizing the properties of all Cys substitutions made in subunit *a* from residues 39–270, including both Ag^+ and NEM sensitivity.

[1] To whom correspondence should be addressed: Dept. of Biomolecular Chemistry, University of Wisconsin, 1300 University Ave., Madison, WI 53706. Tel.: 608-262-1439; Fax: 608-262-5253; E-mail: rhfillin@wisc.edu.

[2] The abbreviations used are: TMH, transmembrane helix; ACMA, 9-amino-6-chloro-2-methoxyacridine; DABMI, 4-dimethylaminophenylazophenyl-4′-maleimide; MTS, methanethiosulfonate; M2M, 1,2-ethanediyl bis-MTS; M4M, 1,4-butanediyl bis-MTS; NEM, *N*-ethylmaleimide; PVDF, polyvinylidene difluoride.

aqueous accessible regions of several membrane proteins. The reagents used, including methanethiosulfonate (MTS) derivatives (20, 21), NEM (22, 23), and Ag^+ (24, 25), react preferentially with the ionized, thiolate form of the Cys side chain and thus can serve as an indicator of the polarity of the environment. Previously we probed Cys residues introduced into the five TMHs of subunit *a* for aqueous accessibility based upon their reactivity with NEM and Ag^+ (26–28). Two regions of aqueous access were found with distinctly different properties. One region extending from Asn-214 and Arg-210 near the center of the membrane to the cytoplasmic surface of TMH4 contains Cys residues that are sensitive to inhibition by both NEM and Ag^+. A second set of Ag^+-sensitive but NEM-inaccessible residues mapped to the opposite face and periplasmic side of TMH4. Ag^+-sensitive but NEM-insensitive residues extending from the center of the membrane to the periplasmic surface were also found in TMHs 2, 3, and 5. The Ag^+-sensitive residues in TMHs 2, 3, 4, and 5 cluster at the interior of the four-helix bundle predicted by cross-linking (19) and could interact to form a continuous aqueous pathway extending from the periplasmic surface to the center of the membrane. In the experiments reported here, we probed the properties of Cys residues introduced at the cytoplasmic boundary of TMH4 and were surprised to discover an extended cytoplasmic region that was sensitive to Ag^+ inhibition. We ultimately introduced Cys substitutions throughout the entire 3–4 loop and then extended mapping to the 1–2 loop. Ag^+-sensitive Cys residues were found at both ends of the 3–4 loop and in the middle of the 1–2 loop. We next asked whether the domains of Ag^+-sensitive residues clustered together and packed near the surface of the membrane by combining Cys substitutions from two domains and testing for cross-linking. The Ag^+-sensitive regions of loops 1–2 and 3–4 proved to be cross-linkable via Cys introduced near the cytoplasmic lipid bilayer interface at the ends of TMHs 3 and 4. We suggest that this Ag^+-sensitive domain(s) may be involved in gating H^+ release to the cytoplasm from the aqueous access channel extending through F_0.

EXPERIMENTAL PROCEDURES

Construction of Cys-substituted Mutants—The cysteine substitutions generated here were transferred into plasmid pCMA113 (26), which contains a hexahistidine tag on the C terminus of subunit *a* and structural genes encoding F_1F_0 subunits from which all endogenous Cys had been substituted by Ala or Ser (29). Cys substitutions were introduced by a two-step PCR method using a synthetic oligonucleotide, which contained the codon change, and two wild type primers (30). PCR products were transferred into pCMA113 directly using unique HindIII (870) or PflMI (1136) and BsrGI (1913) sites (see Ref. 31 for nucleotide numbering). All mutations were confirmed by sequencing the cloned fragment through the ligation junctions. All experiments were performed with the Cys-substituted derivatives of plasmid pCMA113 transformed into the *unc* (*atp*) operon deletion host strain JWP292 (5). All plasmid transformant strains were tested for growth on succinate and glucose as described previously (26).

Membrane Preparation—Plasmid transformants of strain JWP292 were grown in M63 minimal medium containing 0.6% glucose, 2 mg/liter thiamine, 0.2 mM uracil, 1 mM L-arginine, 0.02 mM dihydroxybenzoic acid, and 0.1 mg/ml ampicillin supplemented with 10% LB medium and harvested in the late exponential phase of growth (5). Cells were suspended in TMG-acetate buffer (50 mM Tris acetate, 5 mM magnesium acetate, 10% glycerol, pH 7.5) containing 1 mM dithiothreitol, 1 mM phenylmethylsulfonyl fluoride, and 0.1 mg/ml DNase I and disrupted by passage through a French press at 1.38×10^8 newtons/m^2, and membranes were prepared as described previously (32). The final membrane preparation was suspended in TMG-acetate buffer and stored at −80 °C. Protein concentrations were determined using a modified Lowry assay (33).

ATP-driven Quenching of ACMA Fluorescence—Membranes were suspended in 3.2 ml of HMK-nitrate buffer (10 mM Hepes-KOH, 1 mM $Mg(NO_3)_2$, 10 mM KNO_3, pH 7.5). ACMA was added to 0.3 μg/ml final concentration, and 30 μl of 0.1 M ATP, pH 7.0, was added to initiate quenching of fluorescence. The reaction was terminated by addition of 8 μl of 288 μM nigericin (0.5 μg/ml final concentration). The level of fluorescence obtained after addition of nigericin was normalized to 100% in calculating the percent quenching due to ATP-driven proton pumping. For $AgNO_3$ treatment, 160 μl of membranes at 10 mg/ml were suspended in HMK-nitrate buffer containing 40 μM $AgNO_3$ and incubated at room temperature for 15 min before carrying out the quenching assay. For NEM treatment, membranes at 10 mg/ml in TMG-acetate buffer were treated with 5 mM NEM for 15 min at room temperature and then diluted into HMK-nitrate buffer before carrying out the same quenching assay.

Cross-linking with Bis-MTS Reagents—Cys-substituted membranes were diluted to 10 mg/ml in TMG-acetate buffer at pH 8.5. The bis-MTS reagents M2M and M4M (Toronto Research Chemicals) were dissolved in dimethyl sulfoxide and added to the membranes to a final concentration of 250 μM. The reaction was incubated for 10 min at room temperature and then treated with 5 μl of 0.5 M Na_2EDTA, pH 8.0, and incubated an additional 15 min at room temperature. To reduce and reverse cross-link formation, β-mercaptoethanol was added to a final concentration of 4% by volume, or alternatively dithiothreitol was added to a concentration of 20 mM, and the sample was incubated at room temperature for 15 min prior to dilution into an equal volume of 2× SDS sample buffer (0.125 M Tris, pH 6.8, 4% SDS, 20% (v/v) glycerol) and then incubated at room temperature for 1 h before analysis by SDS-PAGE. Modification by 1 mM DABMI (Molecular Probes Inc.) was also carried out in SDS sample buffer for 1 h prior to SDS-PAGE.

SDS Electrophoresis and Immunoblotting—Samples were run using the SDS-PAGE system described by Laemmli (34). The separating gel contained 15% acrylamide and 0.71% bisacrylamide in 0.375 M Tris at pH 8.8 with 0.125% SDS. The stacking gel was 3% acrylamide and 0.9% bisacrylamide in 0.125 M Tris at pH 6.8 with 0.1% SDS. The running buffer was 0.025 M Tris, 0.192 M glycine, 0.2% SDS adjusted to pH 8.3. The gel was run for 2 h at 75 V through the stacking gel and then for 25 h at a constant 15 mA. Proteins in the separatory gel were transferred to polyvinylidene difluoride (PVDF) membrane by applying 75 V for 1.5 h using 0.192 M glycine, 0.025 M Tris, 20% MeOH buffer adjusted to pH 8.3 (35). Western blotting was performed after

TABLE 1

Functional properties of subunit a substitutions in the 1–2 and 3–4 loops

The properties of substitutions at residues 62, 96–105, 159–164, and 200–203 were also reported elsewhere (28).

Location and mutation	Growth on glucose[a]	Growth on succinate[b]	Quenching with ATP[c]
			%
1–2 loop			
S62C	102	2.5	78 ± 1
V63C	101	2.0	85 ± 1
A64C	100	2.2	82 ± 0
K65C	107	2.2	80 ± 2
K66C	105	2.2	71 ± 2
A67C	100	2.0	77 ± 1
T68C	104	2.0	80 ± 0
S69C	100	2.0	73 ± 4
G70C	101	2.1	67 ± 3
V71C	99	2.1	71 ± 4
P72C	101	2.0	70 ± 6
G73C	108	2.0	73 ± 3
K74C	100	2.2	84 ± 0
F75C	105	2.0	70 ± 7
Q76C	107	2.0	84 ± 1
T77C	103	2.0	69 ± 7
A78C	103	2.0	70 ± 5
I79C	101	2.0	68 ± 4
E80C	99	2.0	84 ± 1
L81C	111	2.0	75 ± 4
V82C	99	1.9	70 ± 5
I83C	108	2.0	75 ± 3
G84C	102	1.8	66 ± 3
F85C	108	2.0	74 ± 1
V86C	102	2.0	68 ± 2
N87C	112	2.0	76 ± 1
G88C	104	2.0	71 ± 1
S89C	99	2.3	71 ± 2
V90C	102	2.3	68 ± 5
K91C	98	2.0	71 ± 2
D92C	105	2.1	66 ± 4
M93C	105	2.0	67 ± 3
Y94C	100	2.1	70 ± 3
H95C	103	2.2	67 ± 6
G96C	112	2.6	77 ± 1
K97C	100	2.1	78 ± 3
S98C	100	2.2	76 ± 2
K99C	111	2.4	76 ± 2
L100C	100	2.2	73 ± 3
I101C	100	2.4	76 ± 1
A102C	105	2.4	74 ± 2
3–4 loop			
I159C	101	2.2	69 ± 4
L160C	100	2.3	64 ± 2
I161C	99	2.3	70 ± 4
L162C	99	2.2	67 ± 2
F163C	99	2.2	69 ± 8
Y164C	88	2.0	74 ± 4
S165C	99	2.1	69 ± 7
I166C	100	2.2	73 ± 0
K167C	99	2.1	74 ± 1
M168C	99	2.4	70 ± 5
K169C	99	2.3	70 ± 5
G170C	99	2.5	73 ± 3
I171C	100	2.6	47 ± 6
G172C	100	2.1	69 ± 4
G173C	101	2.6	69 ± 3
F174C	101	2.4	55 ± 16
T175C	100	2.3	73 ± 5
K176C	100	2.3	70 ± 1
E177C	100	2.1	58 ± 14
L178C	99	2.5	68 ± 3
T179C	99	2.4	70 ± 0
L180C	100	2.3	75 ± 4
Q181C	100	2.1	73 ± 0
P182C	98	2.2	59 ± 5
F183C	99	2.2	74 ± 1
N184C	99	2.4	75 ± 0
H185C	104	2.3	68 ± 1
W186C	100	2.7	65 ± 3
A187C	101	2.7	65 ± 3
F188C	100	2.7	64 ± 0
I189C	101	2.3	64 ± 0
P190C	101	2.5	69 ± 4
V191C	106	2.5	63 ± 5
N192C	99	1.9	42 ± 3
L193C	91	2.2	70 ± 8
I194C	95	2.2	67 ± 5
L195C	94	2.1	59 ± 3
E196C	89	2.0	73 ± 8
G197C	97	2.2	75 ± 6
V198C	92	2.2	74 ± 5
S199C	99	2.3	71 ± 3
L200C	99	2.2	72 ± 3
L201C	99	2.0	73 ± 1
S202C	97	2.2	69 ± 1
K203C	97	2.1	67 ± 2

[a] Yield in liquid minimal medium containing 0.04% glucose expressed as a percentage of growth relative to the cysteine-less control.

[b] Colony size after incubation for 72 h on minimal medium plates containing 22 mM succinate. Colonies from the cysteine-less control strain show average colony sizes of 2.4 ± 0.3 mm.

[c] Measured in a buffer containing 10 mM Hepes-KOH, pH 7.5, 1 mM $Mg(NO_3)_2$, 10 mM KNO_3.

incubation of the PVDF membrane with 5 mg/ml of GE Healthcare Blocking Agent in 1× PBS-Tween (137 mM NaCl, 1.5 mM NaH_2PO_4, 6.5 mM Na_2HPO4, 0.1% Tween 20) for 1 h at room temperature or alternatively overnight at 4 °C. Rabbit antiserum directed against the first 10 amino acids of subunit *a* was preabsorbed to *E. coli* membranes lacking F_0 to reduce immunoartifacts (36). The primary antiserum against subunit *a* was diluted 1:5000 in 1× PBS-Tween with 2% bovine serum albumin and incubated with the PVDF membrane for 1 h at room temperature. Anti-rabbit horseradish peroxidase-linked secondary antibody was diluted 1:40,000 in 1× PBS-Tween and incubated with the PVDF membrane for 1 h at room temperature. The PVDF membrane was incubated for 4.5 min with equal volumes of Super Signal West Pico Chemiluminescent Substrates (Pierce). The PVDF membrane was then exposed to film to visualize the protein.

RESULTS

Properties of Cys Substitutions in Loops 1–2 and 3–4 of Subunit a—In this study, Cys substitutions in the 1–2 and 3–4 loops of subunit *a* were generated in a plasmid encoding subunits of F_1 and F_0 in which the endogenous Cys residues were substituted by Ala or Ser (26). These plasmids were transformed into strain JWP292, which carries a chromosomal deletion of the entire *unc* (*atp*) operon. The growth of these strains on minimal medium was compared using glucose or succinate as a carbon sources (Table 1). The Cys substitutions reported here had minimal effects on growth with either carbon source. Additionally ATP-driven quenching of ACMA fluorescence was performed on inside-out membrane vesicles of the substituted strains to evaluate ATPase-coupled H^+ pumping function (Table 1). The quenching response for most mutants was close to that observed with the control membranes, *i.e.* maximal quenching in the range of 70–80%. Six substitutions at positions 171, 174, 177, 182, 192, and 195 did lead to significant reductions in quenching into a range of 40–60%, but each of these grew nearly as well as wild type via oxidative phosphorylation on succinate minimal medium.

Ag^+ Inhibition of ATPase-coupled H^+ Transport in Cys-substituted 1–2 and 3–4 Loops—Inside-out membrane vesicles with Cys substitutions in the 1–2 or 3–4 loops were treated

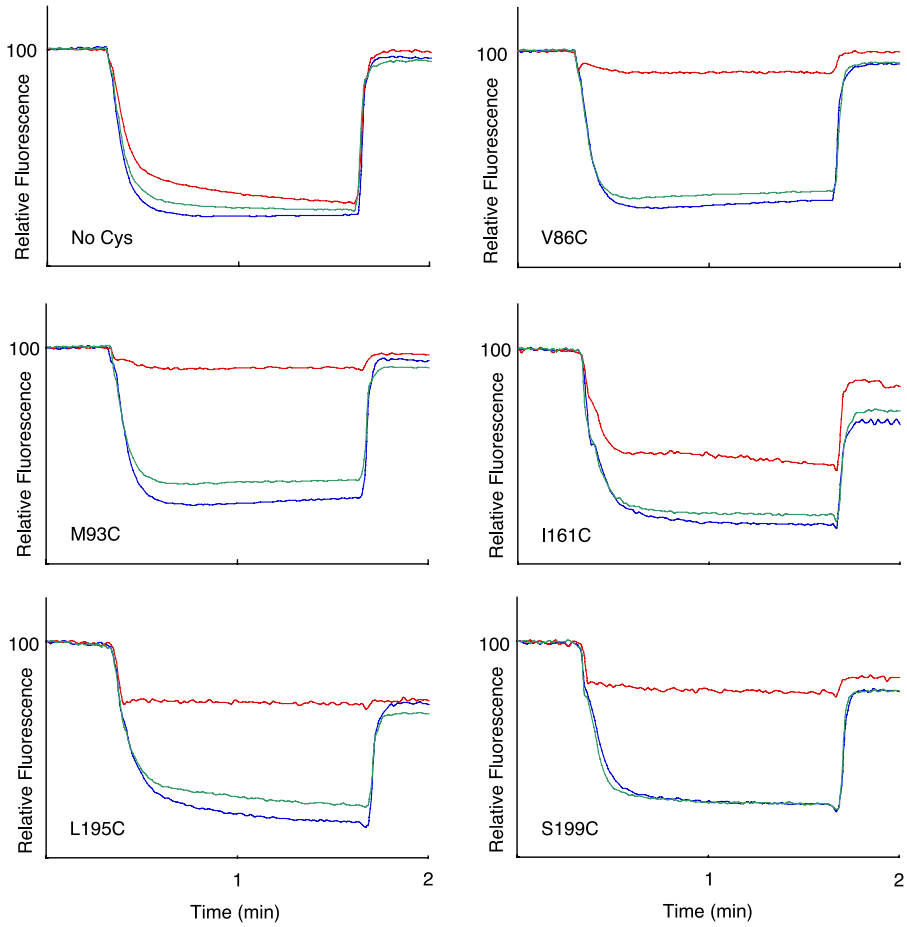

FIGURE 1. **Differing sensitivity of Cys substitutions in 1–2 loop and 3–4 loop to Ag^+ and NEM inhibition.** A 160-μl aliquot of membranes at 10 mg/ml in TMG-acetate were treated with 5 mM NEM for 15 min at room temperature and then diluted into 3.2 ml of HMK-nitrate buffer containing 0.3 μg/ml ACMA. Alternatively membranes were diluted into HMK-nitrate buffer, and $AgNO_3$ was added to 40 μM for 15 min at room temperature prior to addition of ACMA. ATP was added to 0.94 mM at 20 s, and the uncoupler nigericin was added to 0.5 μg/ml at 100 s. The traces indicate no treatment (*blue*), NEM treatment (*green*), or Ag^+ treatment (*red*). The substitution tested is indicated in each panel.

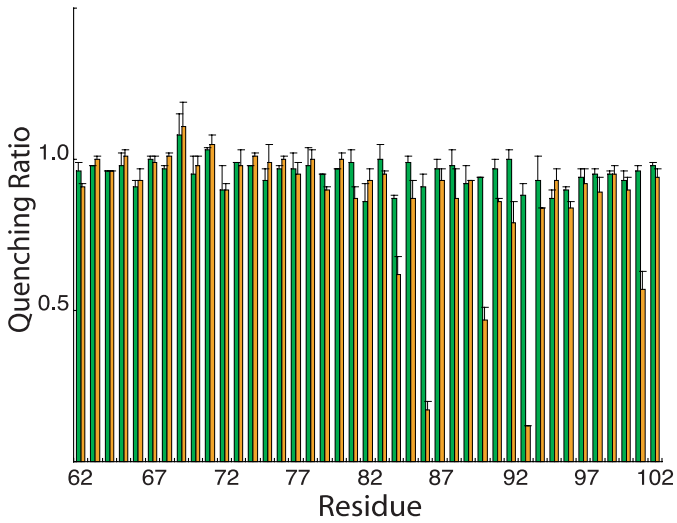

FIGURE 2. **NEM and Ag^+ sensitivity of Cys substitutions in the 1–2 loop.** Results are presented as the ratios of the quenching response in the presence of Ag^+ or NEM to the quenching response in the absence of either reagent. The *green bars* represent the quenching ratio ±NEM treatment, whereas the *orange bars* represent the quenching ratio ±Ag^+ treatment. Each *bar* represents the average ratio from $n \geq 2$ determinations ±S.D.

with 40 μM $AgNO_3$ or 5 mM NEM in chloride-free assay buffer, and the effects on ATPase-coupled H^+ transport were measured by the quenching of ACMA fluorescence. Examples for five Ag^+-sensitive but NEM-insensitive mutants are shown in Fig. 1. In four of the five mutants shown, Ag^+ caused an approximate 90% reduction in the quenching response. In the case of the I161C substitution in loop 3–4, Ag^+ reduced the quenching response by ~50%. In contrast to the observed Ag^+ inhibition, NEM had negligible inhibitory effects on all substitutions examined in this study. The complete surveys of the Ag^+-sensitivity and NEM-sensitivity of cysteine substituted into loops 1–2 and 3–4 are shown in Figs. 2 and 3, respectively. The positions of the Ag^+-sensitive residues in a two-dimensional topological map of subunit *a* are shown in Fig. 4. The most striking distribution of multiple Ag^+-sensitive residues maps to the C-terminal end of loop 3–4 and extends into the cytoplasmic end of TMH4 (Figs. 3 and 4). A single Ag^+-sensitive Cys was found in the middle of loop 3–4. In addition, three cysteines showing moderate sensitivity to Ag^+ (45–50% inhibition) were found at the N-terminal end of loop 3–4. In loop 1–2, Ag^+ sensitivity was confined to three positions in the middle of the loop, *i.e.* residues 86, 90, and 93. The restriction of Ag^+-sensitive Cys to a few localized areas of the loops led us to ask whether the regions interacted physically in the folded structure of the protein and to the cross-linking experiments described below.

The Ag^+-sensitive N- and C-terminal Regions of Loop 3–4 Can Be Cross-linked—To test whether the Ag^+-sensitive N- and C-terminal regions of loop 3–4 interacted with each other, we introduced Cys into both regions and tested for cross-linking with the bis-MTS reagents M2M and M4M. These reagents cross-link between two cysteine sulfhydryls with formation of bis-disulfide bonds and insertion of a -S-$(CH_2)_n$-S-flexible spacer group where $n = 2$ for M2M and $n = 4$ for M4M (21). Cross-link formation was detected by a shift in the mobility of subunit *a* during SDS-PAGE where the cross-linked product shows greater mobility apparently because of a more compact structure (19). The results of several double Cys combinations with the I161C substitution, which demonstrated the 50% inhibition of ACMA quenching by Ag^+ in Fig. 1, are shown in Fig. 5. The general protocol of the experiment is shown in Fig. 5*A* for the I161C/K203C double Cys substitution. The migration of

untreated and β-mercaptoethanol-reduced subunit *a* is shown in *lanes 2* and *3*. When the unmodified double Cys substitution is treated with DABMI (*lane 1*), subunit *a* migrates to a higher apparent molecular weight due to the addition of DABMI molecules to the two Cys residues (DABMI M_r = 320). Treatment with M2M or M4M causes a shift in the subunit *a* band to greater mobility (*lanes 5* and *8*), and the cross-linking prevents subsequent reaction with DABMI in SDS sample buffer (*lanes 4* and *7*). The M2M and M4M cross-linked products are reduced, and the original band migration is restored following treatment with β-mercaptoethanol (*lanes 6* and *9*). The specificity of the reaction is demonstrated in the experiment shown in Fig. 5*B* where neither M2M nor M4M cause cross-linking with the I161C/P204C double Cys substitution. M2M treatment of the I161C/S202C double Cys was concluded to result in partial cross-linking and a smaller shift in mobility of the subunit *a* band; the shifted band was immune to reaction with DABMI (Fig. 5*C*). Similar results, indicative of cross-linking, were seen with the L160C/K203C and I161C/V205C double Cys-substituted mutants (Fig. 5, *D* and *E*). In these cases M2M appears to also react with a minor fraction of the protein to form monovalent adducts, which increase the apparent molecular weight of the protein, without further reaction of the second thiosulfonate group to form a cross-linked product. A summary of results for the double Cys substitutions tested in these areas of the protein is given in Table 2. Cu^{2+}(phenanthroline)$_2$ failed to catalyze cross-link formation with any of the Cys pairs listed in Table 2 that were positive in cross-link with M2M (data not shown).

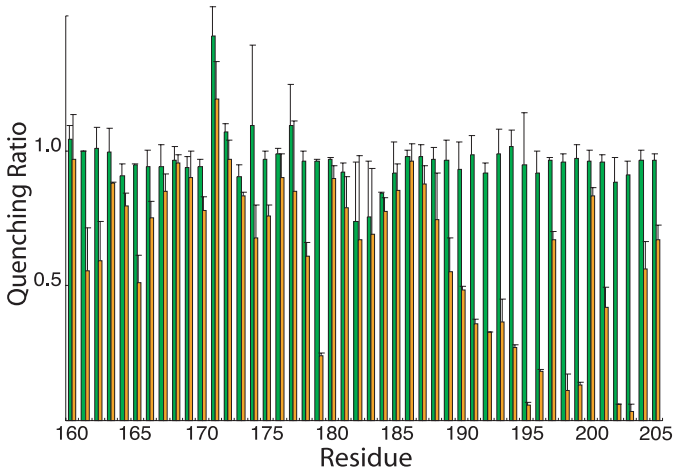

FIGURE 3. **NEM and Ag^+ sensitivity of Cys substitutions in the 3–4 loop.** Results are presented as the ratios of the quenching response in the presence of Ag^+ or NEM to the quenching response in the absence of either reagent. The *green bars* represent the quenching ratio ±NEM treatment, whereas the *orange bars* represent the quenching ratio ±Ag^+ treatment. Each *bar* represents the average ratio from $n \geq 2$ determinations ±S.D.

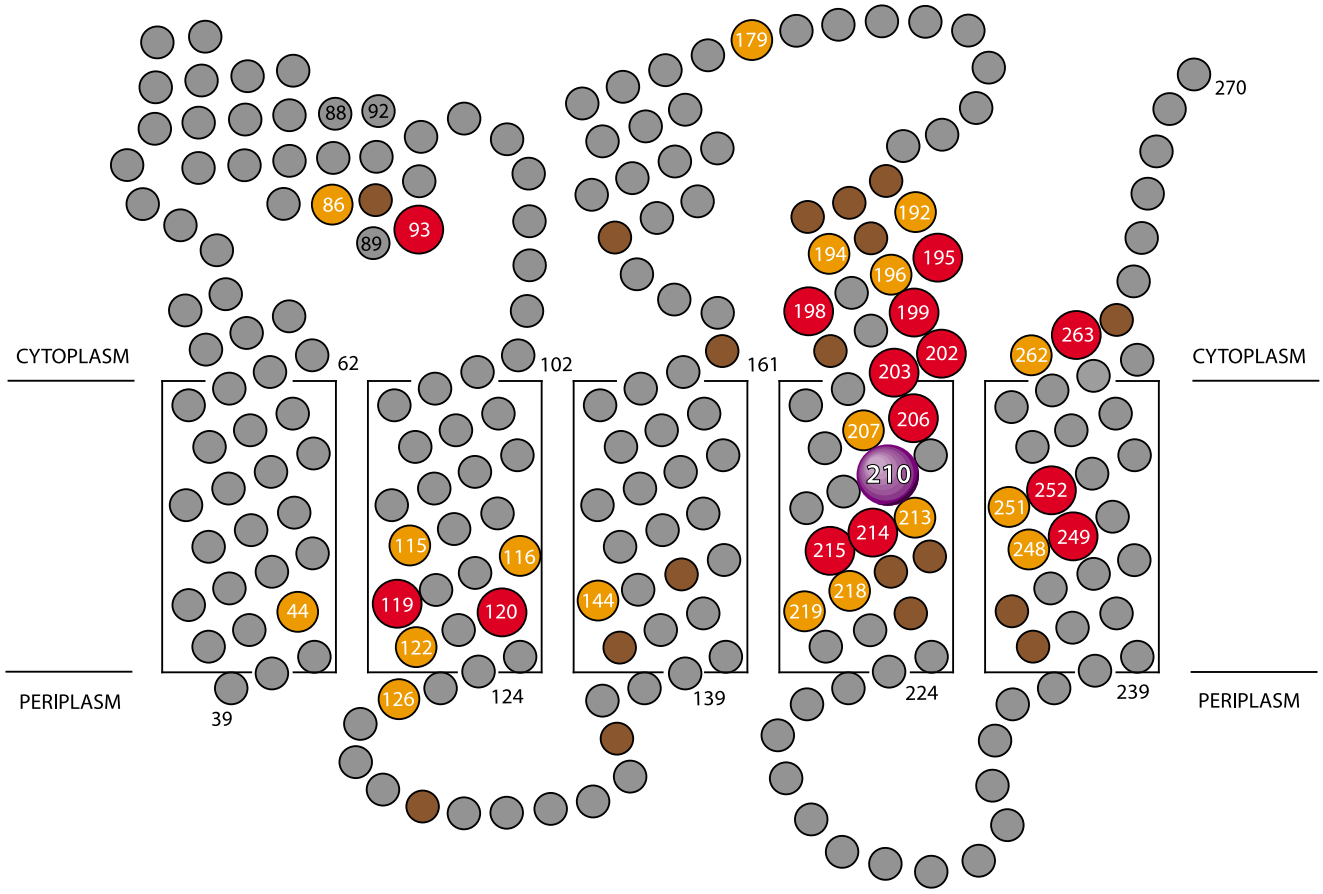

FIGURE 4. **Position of Ag^+-sensitive residues in a two-dimensional topological map of subunit *a*.** The suggested regions of α-helical secondary structure depicted in the 1–2 and 3–4 loops are based upon NMR chemical shift analysis of subunit *a* in chloroform-methanol-H_2O (4:4:1) solvent (53). Residues that are most sensitive to inhibition by Ag^+ are shown in *red* (>85% inhibition), *orange* (66–85% inhibition), and *brown* (46–65% inhibition). The relative depth of placement of the five TMHs of subunit *a* in the lipid bilayer is based upon cross-linking experiments as described elsewhere (19).

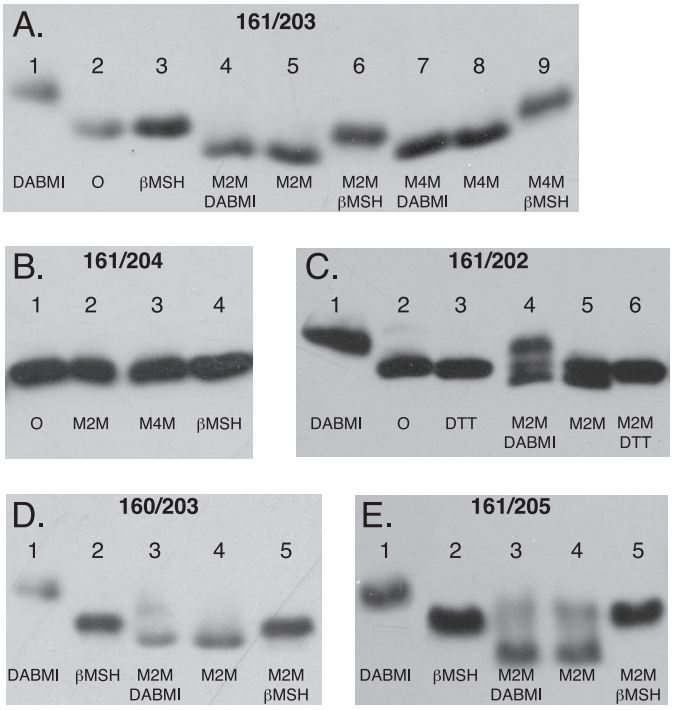

FIGURE 5. **Cross-link formation between pairs of Cys substitutions placed in the two ends of the 3–4 loop.** Membranes from the double Cys substitutions shown were treated with the reagents shown in each lane in the sequence indicated as described under "Experimental Procedures." Following SDS-PAGE, Western blots were probed with anti-subunit *a* antibody. Cross-link formation led to increased electrophoretic mobility and a downward band shift as discussed in the text. *A*, I161C/K203C membranes; *B*, I161C/204 membranes; *C*, I161C/P204C membranes; *D*, L160C/K203C membranes; *E*, I161C/V205C membranes. *βMSH*, β-mercaptoethanol; *DTT*, dithiothreitol; *O*, no treatment.

TABLE 2

Pairs of double Cys substitutions tested for cross-linking between ends of the 3–4 loop

+ indicates cross-link formed after M2M treatment; 0 indicates cross-link not formed after M2M treatment.

Residues at N terminus of loop	Residues at C terminus of loop						
	202	203	204	205	206	207	208
155					0	0	0
157	0	+[a]	0				
158	0	0	0	0			
159	0	0	0	0			
160	0	+	0	+			
161	+	+	0	+			
163		0	0				
165	+	0					

[a] + indicates cross-link formed after M4M treatment but not after M2M treatment.

The Ag^+-sensitive Central Region of Loop 1–2 Can Be Cross-linked to the C-terminal Ag^+-sensitive Region of Loop 3–4—To test whether the Ag^+-sensitive regions in the center of loop 1–2 interacted with the C-terminal Ag^+-sensitive region of loop 3–4, Cys substitutions were introduced into residues in both regions, and the double Cys substitutions were tested for cross-linking with the M2M and M4M. The positive cross-links seen with the V86C/L195C and M93C/L195C double Cys pairs are shown in Fig. 6. Based upon the intensities of the shifted *versus* non-shifted bands in the M2M-treated V86C/L195C sample, ~50% of the subunit *a* was cross-linked. The two Cys residues in the non-cross-linked V86C/L195C band probably reacted monovalently with M2M. This is indicated by the lack of reaction of both M2M-treated sample bands on subsequent treatment with DABMI (*lane 5*). We attempted and were unable to cross-link the Ag^+-sensitive T179C residue in the middle of loop 3–4 with V86C, M93C (not shown), or L195C. The upward shift seen for a fraction of the V86C/T179C and T179C/L195C M2M-treated samples in Fig. 6 is likely due to monovalent M2M adduct formation with the substituted cysteine(s). We were also unable to cross-link V86C or T179C with Y263C, which is positioned at the cytoplasmic end of TMH5 (not shown). Cu^{2+}(phenanthroline)$_2$ failed to catalyze cross-link formation with any of the Cys pairs listed in Table 2 that were positive in cross-link with M2M (data not shown).

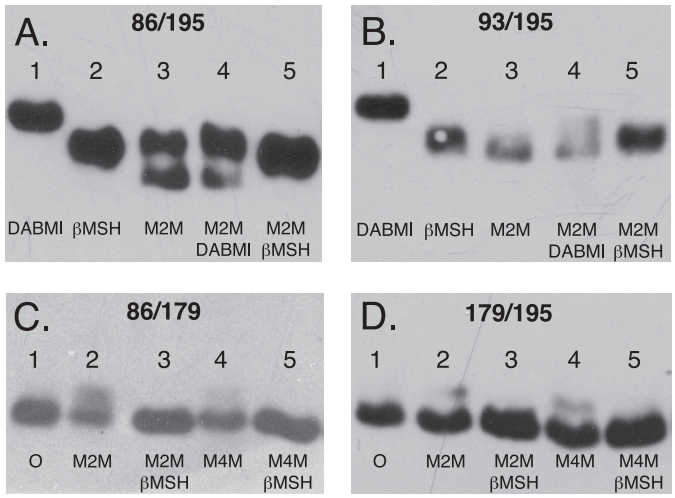

FIGURE 6. **Cross-link formation between Cys substitutions in the center of the 1–2 loop and C-terminal end of the 3–4 loop.** Membranes from the double Cys substitutions were treated with the reagents shown in each lane in the sequence indicated as described under "Experimental Procedures." Following SDS-PAGE, Western blots were probed with anti-subunit *a* antibody. Cross-link formation led to increased electrophoretic mobility and a downward band shift as discussed in the text. *A*, V86C/L195C membranes; *B*, M93C/L195C membranes; *C*, V86C/T179C membranes; *D*, T179C/L195C membranes. *βMSH*, β-mercaptoethanol; *O*, no treatment.

DISCUSSION

Prior to this study, we reported Ag^+-sensitive Cys residues in the five TMHs of subunit *a* that we concluded were likely to be accessed via an aqueous pathway (26–28). As pointed out by others (24), the ionic radius of Ag^+ is close to that of Na^+ or H_3O^+, and hence it may be small enough to permeate water-lined channels. This difference in size may account for its more potent inhibitory properties *versus* NEM as was documented by direct NEM reactivity assays in previous studies (26, 27). In these previous studies, one set of Ag^+- and NEM-sensitive Cys residues was found to cluster on one face on the cytoplasmic side of TMH4 (26) and was proposed to provide an outlet pathway to the cytoplasm (Fig. 4). Other Ag^+-sensitive and NEM-insensitive Cys residues tended to cluster toward the periplasmic side of TMHs 2–5 at the center of a proposed four-helix bundle (26–28), and these interacting helices were proposed to provide an aqueous access pathway from the periplasm to the center of the membrane. In this study Ag^+-sensitive Cys substitutions were found to extend into localized regions of the 3–4 cytoplasmic loop near the surface of the membrane lipid bilayer. The largest set of Ag^+-sensitive residues clustered in a

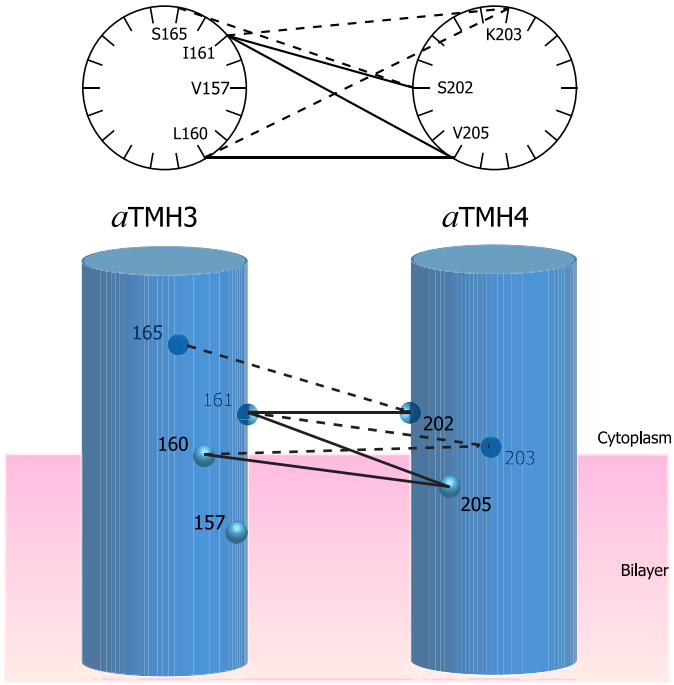

FIGURE 7. **Cross-link formation between modeled α-helical faces of *a*TMH3 and *a*TMH4 as they emerge from the cytoplasmic face of the membrane.** The double Cys pairs that cross-link with M2M are tabulated in Table 2 and here shown connected by *lines*. The *light* or *dark circles* are shown to distinguish the front and back faces of the cylinders. The *solid versus dashed lines* are intended to distinguish cross-linking to the front and back faces of the α-helical *wheels* or *cylinders*. The M4M cross-link between 157 and 203 is not connected by a line.

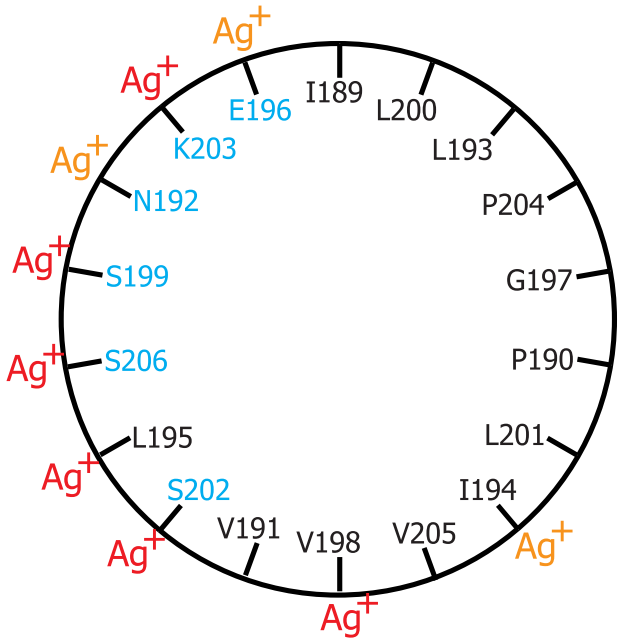

FIGURE 8. **Amphipathic characteristics and Ag^+ sensitivity of residues in an α-helical wheel model for the C-terminal region of the 3–4 loop.** Polar or charged wild type residues are shown in *blue*, and hydrophobic residues are shown in *black*. Ag^+-sensitive Cys substitutions are highlighted with *red* Ag^+ indicating >85% inhibition and *orange* Ag^+ indicating 66–85% inhibition.

span of 12–15 residues at the cytoplasmic end of TMH4 (Fig. 4). A second smaller set of moderately Ag^+-sensitive residues was found at the cytoplasmic boundary extending from TMH3. Finally as the study was expanded, a third set of Ag^+-sensitive residues was found at the center of the 1–2 loop.

The regions of Ag^+-sensitive residues in the 1–2 and 3–4 loops appear to pack within short distances of each other. The packing proximity was indicated by cross-link formation between pairs of Cys introduced at the N- and C-terminal ends of the 3–4 loop and between pairs of Cys introduced in the central region of the 1–2 loop and C-terminal end of the 3–4 loop. The bis-MTS compounds used in these studies would insert short flexible spacers between the cross-linkable Cys pairs, *i.e.* 5.2 Å for the -S-$(CH_2)_2$-S- spacer in M2M (21). Transmembrane helices in other membrane proteins often extend beyond the 30-Å hydrophobic core of the lipid bilayer, and it seems possible that the cross-linkable regions at the ends of the 3–4 loop may be between helical extensions of TMH3 and TMH4 into the head group region of the phospholipid bilayer. The cross-linkable residues are confined to one side of α-helical wheel models for both of these regions (Fig. 7). Cys substituted in TMHs 3 and 4 at positions 148 and 219 at the center of the lipid bilayer can also be cross-linked with Cu^{2+} (19), suggesting that these TMHs are likely to pack in parallel as they extend through the membrane. Cys substitutions in the N-terminal half of the 3–4 loop can be cross-linked to subunit *c* via a bifunctional photoactivable maleimide cross-linker (37), supporting the proximal positioning of this loop region to the surface of the membrane.

The Ag^+-sensitive and cross-linkable region of loop 3–4 extending from Ile-189 to Lys-203 was suggested previously to pack near the cytoplasmic surface of TMH4 (38). In early models for subunit *a*, the region was thought to be transmembrane, and the semiconserved Glu-196 residue was once proposed to form a portion of the proton translocation pathway (39). The region also contains three sites leading to oligomycin resistance in mitochondria at positions equivalent to residues 195, 196, and 199 in *E. coli* (40–42). The other locus encoding oligomycin resistance in yeast mitochondrial subunit *a* maps to a region near His-245 in *a*TMH5 of *E. coli* (42). The other mutations giving rise to oligomycin or venturicidin resistance in yeast mitochondria encircle the equivalent of the Asp-61 residue in *c*TMH2 or lie in residues immediately opposite to Asp-61 in *c*TMH1 (43, 44). Venturicidin resistance mutations have also been mapped to residue 28 in *c*TMH1 of *E. coli* (45). Oligomycin is a hydrophobic and relatively planar, macrocyclic lactone with dimensions of ~10–15 Å (46), and these observations collectively suggest that its binding site may extend from the surface of the membrane in the region of Glu-196 to the area around Asp-61 in the midst of the bilayer. If the region surrounding Glu-196 in loop 3–4 is helical, it would also be amphipathic (Fig. 8), and conceivably the Ag^+-sensitive surface shown in Fig. 8 could interact directly with the Ag^+-sensitive pocket at the cytoplasmic end of TMH5. A possible electrostatic protein interaction at the membrane surface is supported by the unique chemical reactivity of the *a*E196C mutant (12). In the mapping of exposed aqueous accessible loop residues (12), E196C was the only cytoplasmic or periplasmic Cys whose reactivity with membrane-impermeant maleimides was dependent upon treatment with high salt. The region is also resistant to labeling with propionylbiocytin-maleimide (37).

The observation that loop 1–2 residues V86C and M93C can be cross-linked with L195C provides insight into two heretofore unexplained suppressor mutations. Fraga *et al.* (47) isolated a collection of second site suppressor mutations that promoted function of the *c*A24D/D61G aspartate interchange mutant. Of the 23 isolates, 10 mapped to residues in *c*TMH2, and 10 mapped to residues in *a*TMH4. The remaining three isolates mapped to either residue 92 in loop 1–2 or residue 198 in loop 3–4 and, based upon their assumed position in topological models of the protein at that time, provided no insight into how the function of essential Asp in the middle of the membrane was enhanced. The cross-linking results reported here suggest that the Ag^+-sensitive pockets on the cytoplasmic sides of TMHs 4 and 5 and in the 1–2 and 3–4 loops may pack in a single three-dimensional domain, which based upon the second site suppressor studies, could have important interactions with the essential Asp during ATP synthesis.

What possible role could the Ag^+-sensitive regions of loops 1–2 and 3–4 play in F_o function? We suggest that the Ag^+-sensitive regions of the loops may be gating entrance or exit to the cytoplasmic H^+ half-channel leading to Asp-61. Specifically small movements in the loop regions may be coupled to a repositioning of TMHs 4 and 5 to alternatively open and close half-channels to the two sides of the membrane. Movement of the loop positions could be mechanically forced by contacts with the polar loop region of subunit *c* as it moves past subunit *a* during the rotation of the *c* ring. The polar loop could nudge the 3–4 loop to reposition itself such that the connecting TMH4 reoriented itself to allow H^+ in the periplasmic half-channel to access Asp-61. Recall that the periplasmic half-channel is predicted to be at the center of a four-helix bundle, and access from there to the *c* ring surface would require a swiveling of helices at the TMH4/TMH5 interface (27, 28). Once subunit *c* has moved completely past the 3–4 loop region, the loop could relax, and the transmembrane domains could return to their alternate positions. In this orientation Arg-210 on TMH4 would move close to Asp-61 and drive its deprotonation by salt bridge formation. The proton released would exit via the cytoplasmic half-channel extending from Asn-214 and Arg-210 at the center of the membrane to the pocket of Ag^+-sensitive residues at the cytoplasmic surface. Cys residues introduced into this region of TMH4 are both NEM- and Ag^+-sensitive, and this aqueous pocket may extend to the NEM-sensitive V262C substitution at the cytoplasmic face of TMH5 (28).

In suggesting a gating role for the cytoplasmic loop regions of subunit *a* in regulating alternate access of H^+ to Asp-61 from the two sides of the membrane, one is immediately reminded of several elegant, structurally defined examples in other membrane transport proteins. In considering the possible interaction of the 3–4 loop with deeply membrane-embedded regions of TMHs 4 and 5, one remembers the pore helix and selectivity filter in the subunits of the KscA potassium channel that dip into the transmembrane core and then reemerge at the extracellular surface of the membrane (48). The pore helix/selectivity filter region is strongly predicted to be an extracellular loop by hydropathy plot analysis. The sarco/endoplasmic reticulum P-type Ca^{2+}-ATPase provides a perhaps classic example of a moving cytoplasmic domain driving TMH rearrangements to gate ion release (49). A rotational movement of the A (actuator) domain toward the P (phosphorylation) domain is required for dephosphorylation of the E2P intermediate, and the movement is concluded to force the Ca^{2+}-occluding TMHs apart to release Ca^{2+} to the sarcoplasmic reticulum lumen. The cytoplasmic domains of a bacterial Mg^{2+} transporter are proposed to move together and dimerize on Mg^{2+} binding and in so doing change the angle of packing of transmembrane pore helices from the open to closed state to regulate/gate Mg^{2+} entry into the cytoplasm (50). Based upon crystal structures of the Glt_{Ph} Na^+/Asp co-transporter and related co-transporters, a swinging extracellular helical hairpin is proposed to occlude bound Na^+ and substrate and serve as the closed gate prior to TMH movement and gating to open the binding site to the cytoplasm (51). Finally rotation of the four-helix coiled coil, extracellular linker domain in a wide variety of prokaryotic sensory receptors is proposed to be linked to rotation of a membrane-spanning helix to promote transmembrane signaling (52). We thus think that there are ample precedents to speculate that movements of the Ag^+-sensitive cytoplasmic domains of subunit *a* may also provoke changes in the alignment of TMHs 4 and 5 to gate H^+ access and exit from the Asp-61 H^+ binding site in subunit *c*.

Acknowledgments—We thank Hun Sun Chung, Kelly A. G. Herold, and Nick van Gompel for assistance in some of the experiments.

REFERENCES

1. Yoshida, M., Muneyuki, E., and Hisabori, T. (2001) *Nat. Rev. Mol. Biol.* **2,** 669–677
2. Capaldi, R. A., and Aggeler, R. (2002) *Trends Biochem. Sci.* **27,** 154–160
3. Dimroth, P., von Ballmoos, C., and Meier, T. (2006) *EMBO Rep.* **7,** 276–282
4. Senior, A. E. (1988) *Physiol. Rev.* **68,** 177–231
5. Jiang, W., Hermolin, J., and Fillingame, R. H. (2001) *Proc. Natl. Acad. Sci. U. S. A.* **98,** 4966–4971
6. Mitome, N., Suzuki, T., Hayashi, S., and Yoshida, M. (2004) *Proc. Natl. Acad. Sci. U. S. A.* **101,** 12159–12164
7. Meier, T., Polzer, P., Diederichs, K., Welte, W., and Dimroth, P. (2005) *Science* **308,** 659–662
8. Pogoryelov, D., Yu, J., Meier, T., Vonck, J., Dimroth, P., and Muller, D. J. (2005) *EMBO Rep.* **6,** 1040–1044
9. Jones, P. C., Jiang, W., and Fillingame, R. H. (1998) *J. Biol. Chem.* **273,** 17178–17185
10. Dmitriev, O. Y., Jones, P. C., and Fillingame, R. H. (1999) *Proc. Natl. Acad. Sci. U. S. A.* **96,** 7785–7790
11. Fillingame, R., Angevine, C., and Dmitriev, O. (2003) *FEBS Lett.* **555,** 29–34
12. Valiyaveetil, F. I., and Fillingame, R. H. (1998) *J. Biol. Chem.* **273,** 16241–16247
13. Long, J. C., Wang, S., and Vik, S. B. (1998) *J. Biol. Chem.* **273,** 16235–16240
14. Wada, T., Long, J. C., Zhang, D., and Vik, S. B. (1999) *J. Biol. Chem.* **274,** 17353–17357
15. Cain, B. D. (2000) *J. Bioenerg. Biomembr.* **32,** 365–371
16. Hatch, L. P., Cox, G. B., and Howitt, S. M. (1995) *J. Biol. Chem.* **270,** 29407–29412
17. Valiyaveetil, F. I., and Fillingame, R. H. (1997) *J. Biol. Chem.* **272,** 32635–32641
18. Jiang, W., and Fillingame, R. H. (1998) *Proc. Natl. Acad. Sci. U. S. A.* **95,** 6607–6612
19. Schwem, B. E., and Fillingame, R. H. (2006) *J. Biol. Chem.* **281,** 37861–378670

20. Roberts, D. D., Lewis, S. D., Ballou, D. P., Olson, S. T., and Shafer, J. A. (1986) *Biochemistry* **25,** 5595–5601
21. Loo, T. W., and Clarke, D. M. (2001) *J. Biol. Chem.* **276,** 36877–36880
22. Mordoch, S. S., Granot, D., Lebendiker, M., and Schuldiner, S. (1999) *J. Biol. Chem.* **274,** 19480–19486
23. Tamura, N., Konishi, S., Iwaki, S., Kimura-Someya, T., Nada, S., and Yamaguchi, A. (2001) *J. Biol. Chem.* **276,** 20330–20339
24. Lu, Q., and Miller, C. (1995) *Science* **268,** 304–307
25. Li, J., Xu, Q., Cortes, D. M., Perozo, E., Laskey, A., and Karlin, A. (2002) *Proc. Natl. Acad. Sci. U. S. A.* **99,** 11605–11610
26. Angevine, C. M., and Fillingame, R. H. (2003) *J. Biol. Chem.* **278,** 6066–6074
27. Angevine, C. M., Herold, K. A., and Fillingame, R. H. (2003) *Proc. Natl. Acad. Sci. U. S. A.* **100,** 13179–13183
28. Angevine, C. M., Herold, K. A., Vincent, O. D., and Fillingame, R. H. (2007) *J. Biol. Chem.* **282,** 9001–9007
29. Kuo, P. H., Ketchum, C. J., and Nakamoto, R. K. (1998) *FEBS Lett.* **426,** 217–220
30. Barik, S. (1996) *Methods Mol. Biol.* **57,** 203–215
31. Walker, J. E., Saraste, M., and Gay, N. J. (1984) *Biochim. Biophys. Acta* **768,** 164–200
32. Mosher, M. E., White, L. K., Hermolin, J., and Fillingame, R. H. (1985) *J. Biol. Chem.* **260,** 4807–4814
33. Fillingame, R. H. (1975) *J. Bacteriol.* **124,** 870–883
34. Laemmli, U. K. (1970) *Nature* **227,** 680–685
35. Towbin, H., Staehelin, T., and Gordon, J. (1979) *Proc. Natl. Acad. Sci. U. S. A.* **76,** 4350–4354
36. Hermolin, J., and Fillingame, R. H. (1995) *J. Biol. Chem.* **270,** 2815–2817
37. Zhang, D., and Vik, S. B. (2003) *J. Biol. Chem.* **278,** 12319–12324
38. Fillingame, R. H., Jiang, W., Dmitriev, P. C., and Jones, P. C. (2000) *Biochim. Biophys. Acta* **1458,** 387–403
39. Cox, G. B., Fimmel, A. L., Gibson, F., and Hatch, L. (1986) *Biochim. Biophys. Acta* **849,** 62–69
40. John, U. P., and Nagley, P. (1986) *FEBS Lett.* **207,** 79–83
41. Breen, G. A. M., Miller, D. L., Holmans, P. L., and Welch, G. (1986) *J. Biol. Chem.* **261,** 11680–11685
42. Ray, M. K., Connerton, I. F., and Griffiths, D. E. (1988) *Biochim. Biophys. Acta* **951,** 213–219
43. Nagley, P., Hall, R. M., and Ooi, B. G. (1986) *FEBS Lett.* **195,** 159–163
44. Galinis, M., Mattoon, J. R., and Nagley, P. (1989) *FEBS Lett.* **249,** 333–336
45. Fillingame, R. H., Oldenburg, M., and Fraga, D. (1991) *J. Biol. Chem.* **266,** 20934–20939
46. von Glehn, M., Norrestam, R., Kierkegaard, P., Maron, L., and Ernster, L. (1972) *FEBS Lett.* **20,** 267–269
47. Fraga, D., Hermolin, J., and Fillingame, R. H. (1994) *J. Biol. Chem.* **269,** 2562–2567
48. Doyle, D. A., Cabral, J. M., Pfuetzner, R. A., Kuo, A., Gulbis, J. M., Cohen, S. L., Chair, B. T., and MacKinnon, R. (1998) *Science* **280,** 69–77
49. Olesen, C., Picard, M., Winther, A.-M. L., Gyrup, C., Morth, J. P., Oxvig, C., Moeller, J. V., and Nissen, P. (2007) *Nature* **450,** 1036–1042
50. Hattori, M., Tanaka, Y., Fukai, S., Ishitani, R., and Nureki, O. (2007) *Nature* **448,** 1072
51. Boudker, O., Ryan, R. M., Yernool, D., Shimamoto, K., and Gouaus, E. (2007) *Nature* **445,** 387–393
52. Hulko, M., Berndt, F., Gruber, M., Linder, J. U., Truffault, V., Schultz, A., Martin, J., Schultz, J. E., Lupas, A. N., and Coles, M. (2006) *Cell* **126,** 929–940
53. Dmitriev, O. Y., and Fillingame, R. H. (2004) *J. Biomol. NMR* **29,** 439–440